Available online at www.sciencedirect.com
SCIENCE DIRECT
Journal of Catalysis 240 (2006) 58–65
JOURNAL OF CATALYSIS
www.elsevier.com/locate/jcat

Atmospheric pressure studies of selective 1,3-butadiene hydrogenation on well-defined $Pd/Al_2O_3/NiAl(110)$ model catalysts: Effect of Pd particle size

Joaquin Silvestre-Albero, Günther Rupprechter [*,1], Hans-Joachim Freund

Fritz-Haber-Institut, Faradayweg 4-6, 14195 Berlin, Germany

Received 23 December 2005; revised 27 February 2006; accepted 27 February 2006

Abstract

The selective hydrogenation of 1,3-butadiene was studied on a series of $Pd/Al_2O_3/NiAl(110)$ model catalysts with mean Pd particle sizes of 2–8 nm. While Pd nanoparticles $\geqslant$4 nm exhibit a near zero-order reaction kinetics with respect to butadiene, the rate behavior on smaller Pd particles is more complex, and the rate increases with decreasing butadiene pressure. This indicates a change in the rate-limiting step from a regime governed by adsorption to a regime governed by the surface reactions. When the total number of Pd surface atoms is used for rate normalization, the turnover frequency (TOF) of 1,3-butadiene hydrogenation increases linearly with increasing particle size. But this is only an *apparent particle size dependence*. Considering a realistic structural model of the Pd nanoparticles [i.e., with incomplete (111) terraces] for rate normalization, 1,3-butadiene hydrogenation becomes *particle size independent*, even though the reaction is *structure sensitive*, as corroborated by reactivity studies on Pd(111) and Pd(110) single crystals. For 1,3-butadiene hydrogenation, well-faceted Pd nanoparticles $\geqslant$4 nm behave like Pd(111).

Keywords: Selective hydrogenation; Palladium; Nanoparticles; Butadiene; Model catalysts; Size effects

1. Introduction

Control of selectivity is the most important aspect in the hydrogenation of dienes such as 1,3-butadiene. Typically, a high 1-butene/2-butene ratio should be obtained while full hydrogenation to *n*-butane should not occur. For example, in the petrochemical industry, olefins are often produced by catalytic cracking of petroleum and contain significant amounts of dienes [1,2]. Before subsequent processing, these dienes must be selectively converted to 1-butene while hydrogenation of the olefinic stream must be avoided. Pd-based catalysts are widely used for the selective hydrogenation of 1,3-butadiene to 1-butene, due to the high activity and selectivity even in the presence of an excess of olefins [3–6].

Atmospheric pressure studies of selective 1,3-butadiene hydrogenation on Pd(111) and Pd(110) single-crystal surfaces have shown that the reaction is structure sensitive, with the catalytic activity [i.e., the turnover frequency (TOF)] being fivefold higher for the more open (110) surface [7,8]. A higher hydrogen concentration on the Pd(110) surface, due to the higher sticking probability on more open surfaces, was considered responsible for the observed behavior [7,9].

Studies on technical Pd catalysts have shown that the Pd particle size, the support, and the presence of additional transition metals (promoters) have a significant effect on both the catalytic activity and the selectivity of the hydrogenation reaction. For example, for Pd/Al_2O_3 and Pd/SiO_2 powder catalysts, Boitiaux et al. observed an activity decrease with decreasing particle size [10]. A similar conclusion was obtained by Tardy et al. for Pd aggregates supported on activated carbon [11]. This decrease was explained by changes in the electronic structure of small (<3 nm) Pd nanoparticles, leading to stronger interaction with 1,3-butadiene and to stronger deactivation. Unfortunately, the high surface area and porous structure of the powder catalysts often prevented a detailed characterization of the particle surface structure and composition.

* Corresponding author. Fax: +43 1 25077 3890.
E-mail address: grupp@imc.tuwien.ac.at (G. Rupprechter).
[1] Permanent address: Institute of Materials Chemistry, Vienna University of Technology, Veterinärplatz 1, A-1210 Vienna, Austria.

0021-9517/$ – see front matter
doi:10.1016/j.jcat.2006.02.024

The use of clean and well-defined Pd/Al_2O_3 model catalysts [12–14] may be helpful in improving understanding of 1,3-butadiene hydrogenation. In a previous paper we reported results on Pd(111) and Pd(110) [8], and a short account of studies on Pd nanoparticles was reported in [15]. In this paper we present a detailed investigation of particle size effects on 1,3-butadiene hydrogenation, including a description of catalyst structure data. The Pd particle size affects both the kinetic behavior and the reaction selectivity. When the common procedure is used to calculate TOFs, a linear increase is observed for a particle size range of 2–8 nm. However, a detailed characterization of particle size and surface structure by scanning tunneling microscopy (STM) allows us to propose a model that indicates that the TOF is in fact independent of Pd particle size. Pd atoms of incomplete (111) terraces are suggested as active sites. Ultrahigh-vacuum (UHV) studies of olefin hydrogenation on Pd particles and Pd(111) were reported previously [16,17].

2. Experimental

A series of different $Pd/Al_2O_3/NiAl(110)$ model catalysts with Pd particle size ranging from 2 to 8 nm were prepared by evaporation methods under UHV [12,14,18]. First, an ordered Al_2O_3 thin film (around 0.5 nm thick) was grown on a NiAl(110) single crystal by two sequences of oxidation (1×10^{-6} mbar O_2 at 543 K) and subsequent annealing to 1100 K in vacuum [19]. The atomic structure of the Al_2O_3 film was recently characterized by low-temperature (4 K) STM [20]. Pd (99.99%) was then deposited by electron beam evaporation at two different support temperatures, 90 and 303 K. Varying the amount of Pd finally produced different catalysts with mean Pd particle sizes ranging from 2 to 8 nm. Two STM images are shown in Fig. 1 as an inset [13]. (Atomically resolved STM images of individual particles are available elsewhere [21].) As revealed by STM, the as-grown Pd nanoparticles had the shape of truncated cubo-octahedra when the evaporation was carried out at 303 K ($\sim 1 \times 10^{12}$ particles/cm^2), and more disordered particles were seen after evaporation at 90 K ($\sim 5 \times 10^{12}$ particles/cm^2) [19,21]. However, in this study both the 90 and 303 K Pd particles were annealed to 373 K before the reaction, and thus both preparations yielded particles with ordered surfaces. All catalysts prepared exhibited a rather narrow particle size distribution (mean particle size $\pm\sim 1$ nm).

Once a $Pd/Al_2O_3/NiAl(110)$ catalyst was prepared, the sample was transferred under UHV to a high-pressure reaction chamber attached to the UHV system [8,14,18]. Kinetic measurements of 1,3-butadiene hydrogenation were performed at atmospheric pressure (reaction mixture: $P_{1,3\text{-butadiene}}$, 5 mbar; P_{H_2}, 10 mbar; Ar added up to 1 bar) at 373 K. At this (high) reaction temperature and low hydrogen pressure, the formation of β-Pd-hydride (requiring at least 200 mbar H_2) can be excluded. Kinetic measurements were done in batch mode with the gas recirculated over the catalyst by a metal bellows pump (reactor volume 755 cm^3 exchanged 4 times/min) and were reproducible within 5%. Reaction products were analyzed by on-line gas chromatography (GC), using a $HP\text{-}PLOT/Al_2O_3$ (50 m × 0.53 mm) capillary column and a flame ionization detector. Retention times and sensitivity factors for the reactant and the products were calibrated using a number of different gas mixtures. The absence of background (wall) reactions under typical operating conditions was confirmed using Al_2O_3 films on NiAl(110) as "inert" catalysts.

Under the relatively "mild" reaction conditions, structural changes of the Pd nanoparticles can be mostly excluded. Postreaction surface characterization by chemisorption or vibrational spectroscopy (using CO as probe molecule) did not indicate any surface restructuring, such as particle sintering or strong surface structure changes. Furthermore, repeated kinetic measurements after several hours of reaction time showed only very small variations. Surface restructuring *during* the reaction cannot be fully excluded but is unlikely, because it must have been fully reversible.

Pd(111) and Pd(110) single crystals ($\varnothing \sim 10 \times 2$ mm) were used as reference samples [8]. The crystals were cleaned by annealing to 1100 K, Ar ion etching (beam voltage 900 V at 6×10^{-6} mbar Ar at 298 K), heating to 1100 K, oxidation during cooling down in 5×10^{-7} mbar O_2 between 1100 and 600 K, and a final flash to 1100 K in UHV. After cooling to 90 K, well-ordered and clean surface structures were confirmed by LEED and CO-TPD. For the single-crystal Pd, atoms on both surfaces [front and back; both of (111) orientation] and on the perimeter were considered for the TOF calculations, because carbon impurities easily dissolve in Pd on flashing above 700 K.

3. Results and discussion

3.1. Catalytic behavior

3.1.1. Rate measurements

Figs. 1a–1e show the reaction kinetics of 1,3-butadiene hydrogenation at 373 K for different Pd catalysts with 2–8 nm mean particle size. For all samples, independent of Pd particle size, 1-butene, *trans*-2-butene, and *cis*-2-butene were the primary products, with the thermodynamically least stable 1-butene being the main product (100% selectivity toward butene formation). Interestingly, in the first minutes of the reaction (before complete butadiene consumption), the relative proportion of these three products was quite independent of particle size; that is, a 1-butene/2-butene ratio of around 1.3 and a *trans*-/*cis*-2-butene ratio of around 3.4 were observed. The similarity in the relative amount of the three reaction products points to an identical reaction mechanism for the (first) butadiene hydrogenation step on the different Pd clusters, that is, independent of particle size, most probably through 1,2- and 1,4-H addition to 1,3-butadiene to produce 1-butene and *trans*-/*cis*-2-butene, respectively [8,22]. Although the product distribution followed a similar trend for all particle sizes examined, the kinetic behavior was clearly size dependent (Fig. 1). For the smallest particle size (2 nm; Fig. 1a), the catalytic activity increased with reaction time. In fact, at high butadiene pressure (i.e., low reaction time), the catalyst exhibited a constant activity. However, after the butadiene pressure was reduced to a certain value ($\sim$30% butadiene conversion), the activity suddenly increased until 1,3-butadiene was completely

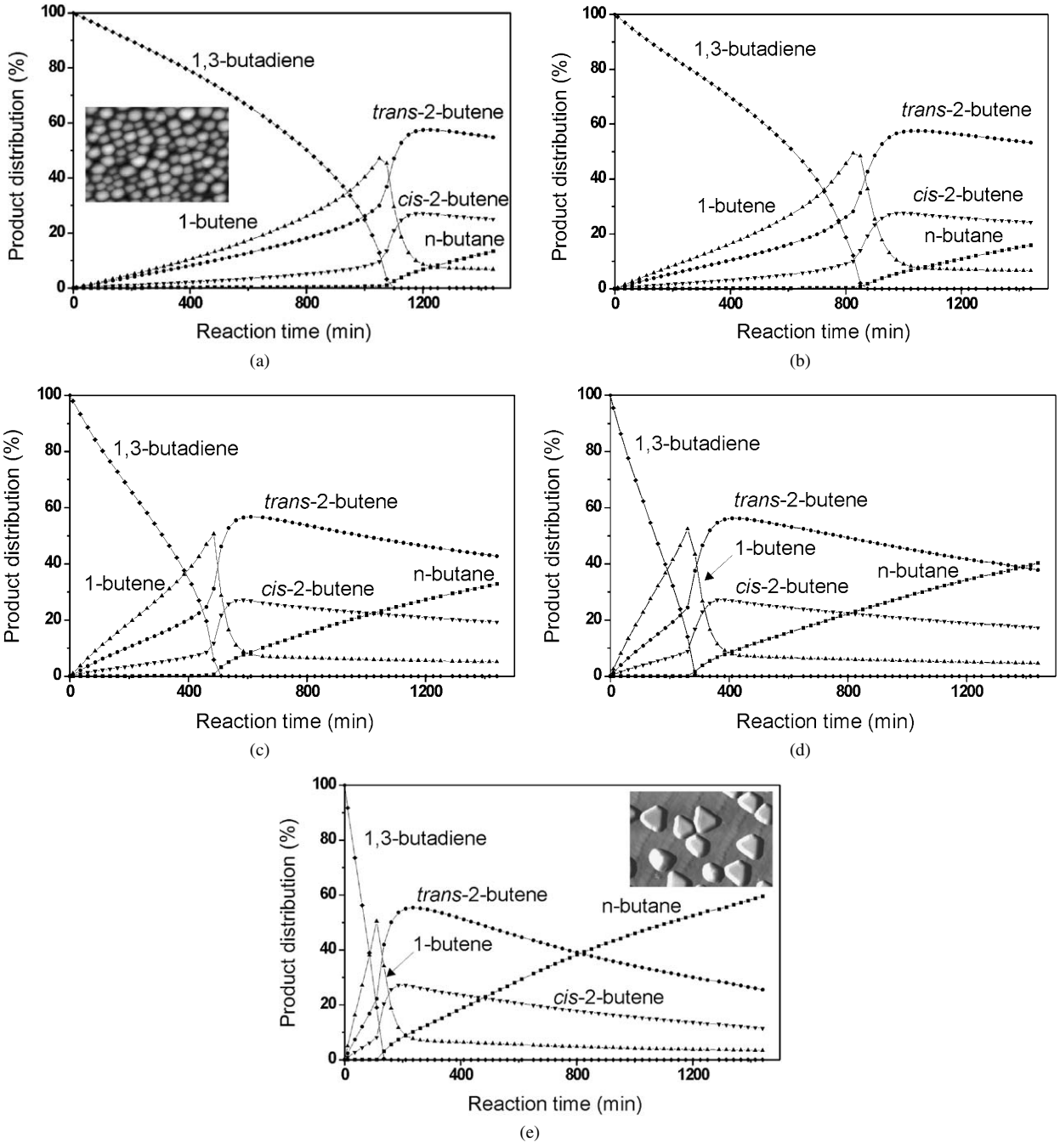

Fig. 1. Product distribution versus reaction time for 1,3-butadiene hydrogenation at 373 K for different $Pd/Al_2O_3/NiAl(110)$ model catalysts ($P_{1,3\text{-butadiene}}$: 5 mbar; P_{H_2}: 10 mbar; Ar added up to 1 bar): (a) mean particle size 2.1 nm (2 Å, 90 K), (b) 4.2 nm (2 Å, 303 K), (c) 5.3 nm (4 Å, 303 K), (d) 6.1 nm (6 Å, 303 K), and (e) 7.7 nm (12 Å, 303 K).

consumed. Such a behavior resembles a transition from an adsorption/desorption-limited regime to a kinetic regime (rate governed by the surface reactions). In fact, when the experiment of Fig. 1a was performed with an initial butadiene pressure of 3.5 mbar (i.e., 70% of the original concentration in Fig. 1a), the reaction rate increased already from the beginning, confirming the importance of the hydrocarbon coverage (or pressure). Apparently, when the butadiene coverage (pressure) was above a "critical" value, the strongly adsorbed butadiene (fully) covered the Pd particle surface and inhibited hydrogen adsorption. Under these conditions, the activity was governed by adsorption/desorption processes; when a butene molecule, originating from the hydrogenation of butadiene, desorbed from the surface, an empty site was created, allowing hydrogen to access the Pd surface and "perforate" the hydrocarbon layer. This assumption is supported by hydrogen–deuterium exchange experiments on Pd/Al_2O_3 catalysts showing that the presence of 1,3-butadiene inhibited HD formation [3,23]. However, with reaction time, the partial pressure of butadiene continuously decreased, and below a critical coverage, hydrogen was able to (better) perforate the hydrocarbon layer, eventually leading to progressively increasing catalytic activity.

As mentioned above, evaporation at 303 K allowed the preparation of larger Pd particles, between 4 and 8 nm mean size. Fig. 1b shows that the overall kinetic behavior for the 4-nm sample was similar to that of the 2-nm Pd–Al_2O_3 catalyst. Again, the 4-nm catalyst exhibited a critical hydrocarbon pressure/coverage below which the catalytic activity suddenly increased (after 500 min; Table 2). The Pd particles of the 4-nm catalyst (Fig. 1b) had twice the diameter of those of the 2-nm catalyst, but, due to the smaller island density after evaporation at 303 K, the number of Pd surface atoms was ∼50% of those of the 2-nm catalyst (see Table 1). However, it is interesting to note that although the number of Pd surface atoms was smaller (∼50%) for the 4-nm catalyst than for the 2-nm catalyst, 1,3-butadiene consumption was faster for the 4-nm catalyst (complete consumption after 850 min) than for the 2-nm catalyst (complete consumption after 1100 min). This indicates that the overall activity increased with increasing particle size (cf. Figs. 1a and 1b). When 4-nm Pd particles were grown at 90 K, the higher island density led to a ∼380% increase in the number of Pd surface atoms compared with the catalyst of Fig. 1b. Accordingly, the overall consumption of 1,3-butadiene was faster (complete consumption after 200 min; not shown).

Table 1
Structure properties of different Pd/Al_2O_3/NiAl(110) model catalysts

Substrate temperature during evaporation (K)	Pd nominal thickness[a] (Å)	Island density[b] (cm^{-2})	Mean particle diameter[c] (nm)	Dispersion[c] (%)	Total number of Pd surface atoms[d]
90	2	$8.7 \cdot 10^{12}$	2.1	61	$7.6 \cdot 10^{14}$
90	4	$6.3 \cdot 10^{12}$	2.8	43	$1.1 \cdot 10^{15}$
90	6	$4.7 \cdot 10^{12}$	3.6	34	$1.3 \cdot 10^{15}$
90	8	$3.6 \cdot 10^{12}$	4.4	29	$1.4 \cdot 10^{15}$
303	2	$1 \cdot 10^{12}$	4.2	30	$3.7 \cdot 10^{14}$
303	4	$1 \cdot 10^{12}$	5.3	24	$5.9 \cdot 10^{14}$
303	6	$1 \cdot 10^{12}$	6.1	21	$7.7 \cdot 10^{14}$
303	12	$1 \cdot 10^{12}$	7.7	16	$1.2 \cdot 10^{15}$

[a] Values measured by a quartz microbalance thickness monitor.
[b] Values obtained by in situ STM measurements [19].
[c] Values calculated based on the deposited Pd amount and the island density measured by STM.
[d] For a sample area of 0.92 cm^2.

An increase in Pd particle size from 4 to 8 nm had an important effect on catalytic activity (Figs. 1b–1e). With increasing size, 1,3-butadiene consumption became more linear, with the 8-nm particles *approaching* the zero-order reaction kinetics of a Pd(111) single crystal with respect to butadiene [8]. Although the initial butadiene pressure was always 5 mbar, the site-blocking effects on activity could hardly be recognized for large particles, even for low conversions (when blocking effects were observed for small particles). When the island density was kept constant (evaporation at 303 K), an increase in Pd particle size apparently led to a threefold increase in the total number of Pd surface atoms (Table 1), but this alone cannot explain the kinetic behavior, again suggesting site-blocking. For Pd single crystals, the blocking effects were basically absent for the current conditions (see Fig. 3a of [8]).

According to these results, 1,3-butadiene adsorbed on Pd nanoparticles hindered hydrogen adsorption, and this effect was more pronounced for small Pd particles. This could be due in part to a more rapid reduction of blocking effects for larger particles, because of the threefold to fourfold greater number of Pd surface atoms (Table 1). However, the butadiene conversion (or pressure) at the point where the kinetics change differed for the different catalysts, ruling out the possibility that the faster reaction on larger particles was simply masking the blocking effects (see Table 2). In fact, although the catalysts in Figs. 1a (2 nm) and 1d (6 nm) exhibited basically the same total number of Pd surface atoms, their kinetic behavior was quite different. Whereas the 6-nm particles exhibited a fast reaction rate already from the beginning, the 2-nm Pd particles seemed to suffer from blocking effects during most of the reaction. This clearly shows that the complex kinetic behavior on Pd nanoparticles was not governed simply by the actual butadiene coverage (pressure), but there was a size-dependent adsorption of butadiene that was stronger on small Pd particles. This finding is in good agreement with previous spectroscopic studies on Pd aggregates that reported a change in the electronic properties of small Pd particles and a stronger adsorption of butadiene on small Pd particles, which was responsible for the activity decrease with decreasing particle size [11,24]. Table 2 shows the partial pressure of 1,3-butadiene at the point where the reaction kinetics accelerated. A comparison of this pressure for differ-

Table 2
Kinetic measurements on different Pd/Al_2O_3/NiAl(110) model catalysts for selective 1,3-butadiene hydrogenation at 373 K

Catalysts	Particle size (nm)	Selectivity[a] (%)				1-Butene/2-butene[a]	Selec. butene[a] (%)	TOF (s^{-1})	P_{HC}[b] (mbar) (conversion (%))
		1-Butene	*Trans*-2-butene	*Cis*-2-butene	*n*-Butane				
2 Å, 90 K	2.1	52.5	36.4	10.3	0.8	1.12	99.2	1.1	3.6 (28)
4 Å, 90 K	2.8	51.4	37.8	10.2	0.6	1.07	99.4	2.0	2.3 (54)
6 Å, 90 K	3.6	54.8	34.2	10.7	0.3	1.22	99.7	3.6	1.8 (64)
8 Å, 90 K	4.4	56.0	32.9	11.0	0.2	1.28	99.8	4.0	1.3 (74)
2 Å, 300 K	4.2	55.2	33.4	10.8	0.6	1.25	99.4	3.7	3.1 (38)
4 Å, 300 K	5.3	57.9	31.2	10.5	0.4	1.39	99.6	5.3	2.1 (58)
6 Å, 300 K	6.1	60.6	29.6	10.6	0.2	1.54	99.8	7.0	0.7 (86)
12 Å, 300 K	7.7	61.9	27.7	10.3	0.1	1.63	99.9	9.6	–

[a] Measured at 50% conversion ($P_{1,3\text{-butadiene}}$: 5 mbar; P_{H_2}: 10 mbar; Ar added up to 1 bar).
[b] Partial pressure (and conversion) of 1,3-butadiene when the reaction rate accelerates.

ent Pd particle sizes is not straightforward and is not discussed here.

For all catalysts, once 1,3-butadiene was completely consumed, 1-butene was readsorbed on the Pd catalyst, giving rise to two processes: *n*-butane formation through hydrogenation and *trans*-/*cis*-2-butene formation through isomerization. Interestingly, the kinetics of the 1-butene reaction (hydrogenation and isomerization) were similar for the different catalysts and thus independent of the Pd particle size (Fig. 1). In fact, on small (2 nm) Pd particles, the 1-butene reaction did not exhibit the typical blocking effects observed for butadiene hydrogenation. For all particle sizes, the kinetics of 1-butene reaction were fast from the beginning, pointing to a weaker adsorption of 1-butene on Pd nanoparticles compared with 1,3-butadiene (in agreement with recent density functional theory calculations [25–27]). This suggests that in the case of 1,3-butadiene, both double bonds were interacting with the surface, explaining the stronger bonding. The interaction with both double bonds is further corroborated by the reaction selectivity observed on Pd single crystals (suggesting that both 1,2- and 1,4-hydrogenation occurred, as discussed in detail previously [8]).

3.1.2. Selectivity to butenes

The hydrogenation of 1,3-butadiene is also interesting with respect to the reaction selectivity (with the products 1-butene, *trans*-2-butene, *cis*-2-butene, and *n*-butane). As mentioned before, the relative fraction of the different reaction products was quite similar for the different $Pd/Al_2O_3/NiAl(110)$ model catalysts. However, as shown in Table 2, small but noticeable differences occurred as a function of Pd particle size. An increase in particle size from 2 to 8 nm induced a small increase in the selectivity toward 1-butene (and a small increase in the selectivity toward butenes in general). Apparently, larger Pd nanoparticles exhibited higher activity (TOF) for 1,3-butadiene as well as slightly higher selectivity for 1-butene. This may suggest that on larger particles, 1,2 hydrogen addition was faster than 1,4 hydrogen addition; however, the precise origin of this effect (e.g., particle size-dependent binding energy of intermediates) is currently unknown.

A more pronounced difference was observed between Pd nanoparticles and Pd single crystals [8]. For Pd nanoparticles, the selectivity toward butene formation was considerably higher; that is, no *n*-butane was formed until 1,3-butadiene had been completely consumed, whereas on Pd single crystals, small amounts of *n*-butane were formed even in the presence of 1,3-butadiene. The higher selectivity of Pd nanoparticles may again be related to a stronger adsorption of butadiene on the particles, preventing butene readsorption and *n*-butane formation.

3.2. Effect of Pd particle size: structural considerations

Table 1 collects the structural characteristics of the different Pd catalysts, focusing on particle properties. On evaporation at low temperature (90 K), Pd particle size ranged from approximately 2 to 4 nm, whereas larger particles (4–8 nm) resulted on evaporation at room temperature. Taking into account the amount of deposited Pd (Pd atoms per cm^{-2}, measured with a quartz microbalance) and the island density (Pd particles per cm^{-2}) determined by in situ STM [19], we can calculate such structural characteristics as Pd atoms per particle, mean particle size, and dispersion. In what follows we use these structural properties to correlate the catalytic activity with the microscopic properties of the catalysts.

All measurements described in the previous section were performed on different catalysts, that is, with different particle sizes and different numbers of Pd surface atoms. These differences make a direct comparison of kinetic behavior difficult. Using the TOF (i.e., number of molecules reacted per Pd surface atom after a certain time) allows a better comparison of rates for different particle sizes; this concept is frequently used in heterogeneous catalysis. Accordingly, Table 2 also reports TOF values after 60 min of reaction time as a function of Pd particle size. TOF values for the different catalysts were calculated by dividing the total number of product molecules (1-butene, *trans*-2-butene, *cis*-2-butene, and *n*-butane) produced after 60 min of reaction time by the corresponding number of Pd surface atoms (Table 1).

The catalytic activity increased linearly with particle size (see also Fig. 3b). Apparently, Pd surface atoms on larger particles were more active than those on small particles. This tendency agrees with previous results for 1,3-butadiene hydrogenation on Pd aggregates showing an exponential TOF increase with particle size [11]. This behavior can be explained by a stronger deactivation on small Pd particles (1.2–2.8 nm) due to stronger butadiene adsorption; variations in electronic structure were observed for Pd particles <3 nm. However, this explanation cannot be extrapolated to particle sizes up to 8 nm, and additional effects must be considered. Previous studies of 1,3-butadiene hydrogenation on Pd single crystals have shown that the reaction is *structure sensitive*; that is, the catalytic activity depends on the crystallographic orientation of the surface; as mentioned, Pd(110) is fivefold more active than (111) [7,8]. Taking into account that the Pd nanoparticles exhibit facets of different crystallographic orientation [e.g., (111) and (100)], variations in the relative abundance of the different facets with particle size will also affect the overall catalytic activity (because the different facets exhibit different activity).

In addition, for small Pd nanoparticles (Fig. 1a), there were clear differences between 1,3-butadiene hydrogenation (first hydrogenation reaction) and 1-butene hydrogenation (consecutive hydrogenation reactions). Whereas the hydrogenation of a C_4 molecule with two conjugated double bonds, such as 1,3-butadiene, exhibited hydrogen-blocking effects, a similar C_4 molecule with only a single double bond, such a 1-butene, did not show these effects. This difference points to special site requirements (i.e., structure sensitivity) for 1,3-butadiene adsorption and hydrogenation.

As mentioned in Section 2, Pd nanoparticles were prepared under UHV on a thin oxide support that allowed characterization by STM [13,19]. STM imaging showed that the Pd nanoparticles had a truncated cubo-octahedral shape with (111) and (100) surface facets (cf. the model in Fig. 2a). Based on this information, we constructed a cubo-octahedral cluster model

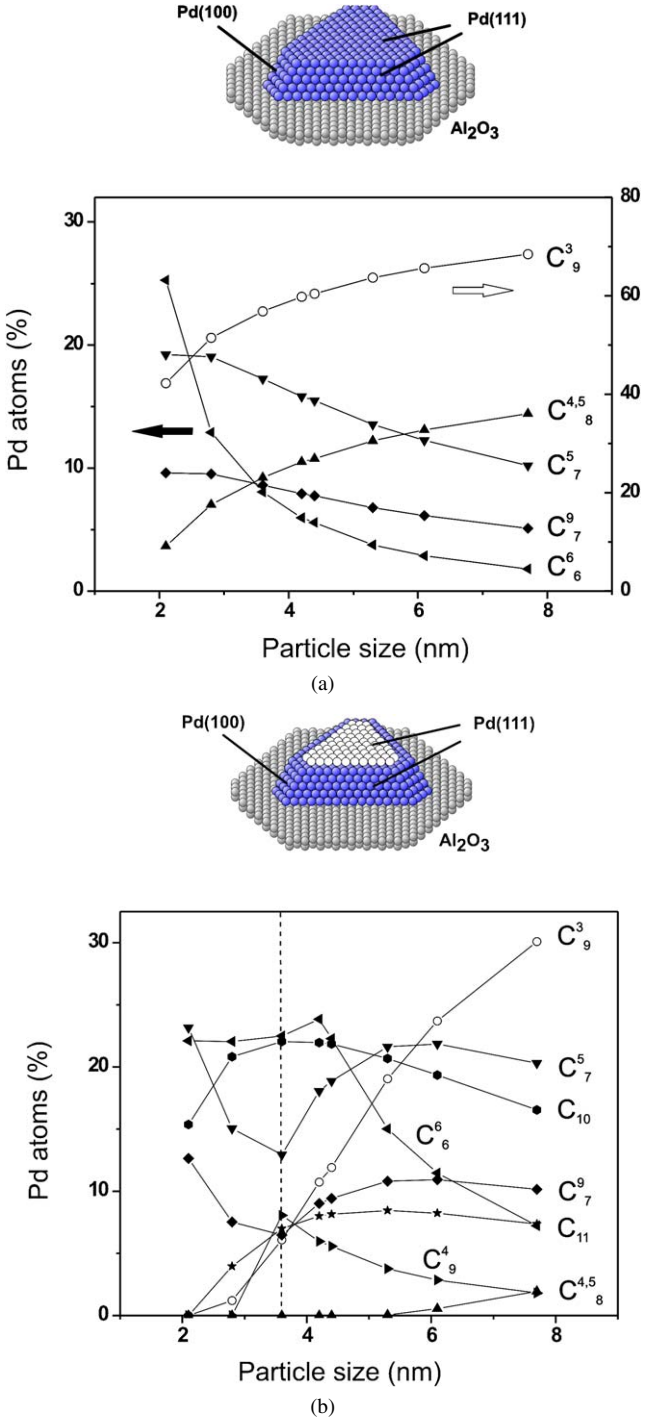

Fig. 2. Relative abundance of Pd surface atoms in different configurations, considering (a) perfect truncated cubo-octahedra and (b) truncated cubo-octahedra with incomplete (111) and (100) terraces (incomplete layers on side facets are not shown for graphical reasons).

that allows us to split the total number of surface Pd atoms into the different contributions of the (111) and (100) surface facets, edge sites, interface sites, and so on. Fig. 2a shows the relative abundance of surface sites as a function of the Pd particle size for truncated cubo-octahedral clusters [i.e., for perfect (closed-shell) cubo-octahedra]. The following site notation is based on that suggested by Van Hardeveld and Hartog; that is, the subscript and the superscript correspond to the number of nearest neighbors of a surface atom and to the serial numbers of the missing atoms in the neighborhood of a certain surface atom, respectively. (Full coordination would be 12; see Fig. 1 in [28] for a complete description.) Small metal clusters had a high proportion of corner (C_6^6) and edge (C_7^5 and C_7^9) atoms compared with atoms in (111) and (100) terrace sites, C_9^3 and $C_8^{4,5}$, respectively. However, an increase in particle size led to an increase in the proportion of (111) and (100) terraces; for 8-nm particles, around 70% of the surface atoms were within (111) terraces and 15% were within (100) terraces.

The STM images also revealed that the Pd particles were not always perfect cubo-octahedra but frequently exhibited *incomplete* (111) and (100) terraces; that is, a few atom rows were missing at the border/intersection of the (111) and (100) facets. Therefore, we also used a second structural model with incomplete facets (Fig. 2b). Because of the greater number of different surface sites on the particle, the graph is more complex, but it can be split in two main parts. The small (<3.5 nm) metal clusters were highly defective, and a slight increase in particle size led to an increase in the proportion of defects at the boundary of the incomplete facets (mainly C_{10}, C_{11}, and C_9^4). In contrast, particles >3.5 nm started to develop large and well-defined (111) facets (i.e., C_9^3) and (100) facets (i.e., $C_8^{4,5}$); consequently, a sudden change in the fraction of the different sites occurred, as shown in Fig. 2b. It is noteworthy that the proportion of well-defined (100) terraces in the cubo-octahedral model with incomplete terraces was as low as 2% for the 8-nm particles.

Considering that the hydrogenation reaction occurred on specific surface sites and assuming that the morphology and proportion of these sites remained unchanged under high-pressure reaction conditions (which is justified by the arguments given in Section 2), we plotted the increase in *absolute* catalytic activity (molecules reacted/s) with particle size together with the increase in the *total* number of a certain type of Pd sites with particle size for both perfect and incomplete cubo-octahedra (Fig. 3a). Comparing these two dependences reveals that the hydrogenation activity increased in basically the same manner as the number of Pd atoms in incomplete (111) terraces increased (Fig. 3a). We do not show plots for other surface sites [e.g., (100), edges], because no correlation was observed.

In the next step, the number of Pd atoms in incomplete (111) terraces was used for the rate normalization, yielding a TOF that was constant for Pd particles ⩾4 nm (Fig. 3b). According to this finding, the selective hydrogenation of 1,3-butadiene was *particle size independent* for Pd particles ⩾4 nm, although the reaction itself was structure sensitive. This indicates that for large Pd particles, the reaction occurred on (111) terraces, which may be required for a specific diene adsorption geometry. If this assumption were true, then one would expect a similar TOF for a Pd(111) single crystal. Therefore, the catalytic activity of Pd(111) was measured under the same reaction conditions. As shown in Fig. 3b (arrows on the left), the TOF for 1,3-butadiene hydrogenation on Pd(111) was very close to that observed for Pd nanoparticles (only 3–6 s^{-1} = 16%

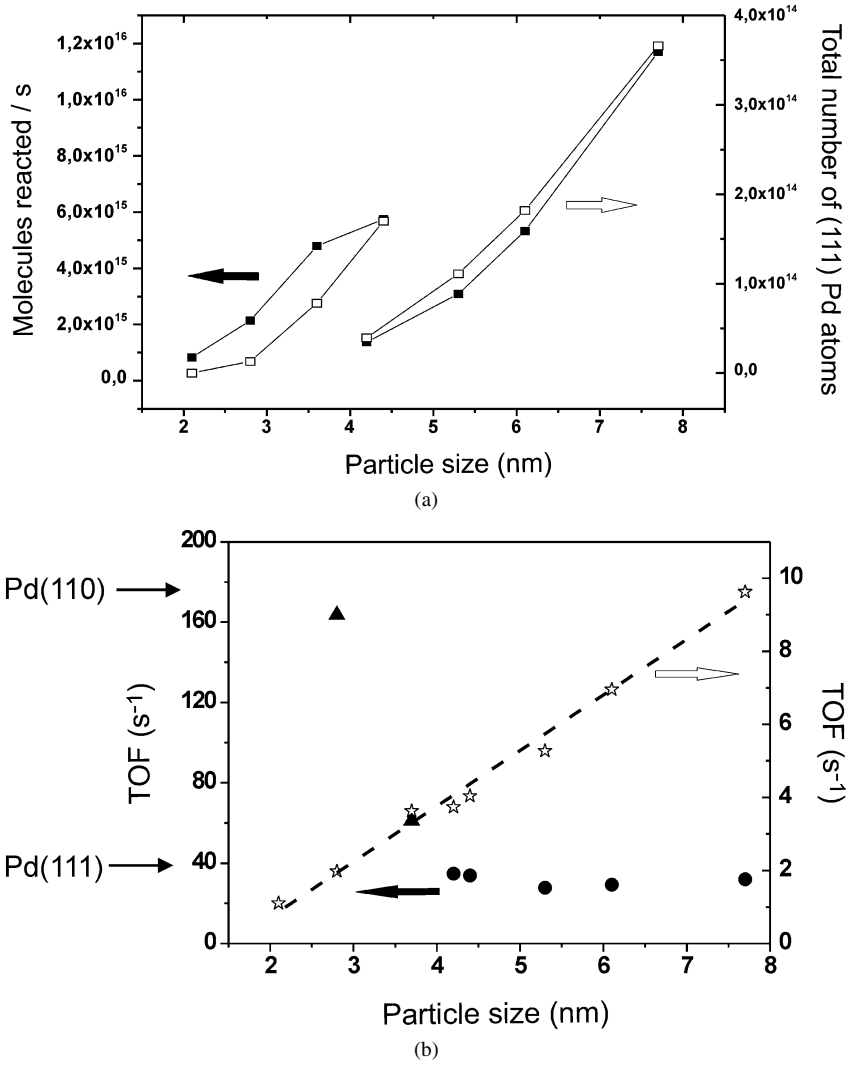

Fig. 3. (a) Catalytic activity (molecules converted/s; ■) and total number of Pd atoms in incomplete (111) terraces (□), both as a function of Pd particle size; (b) specific activity (TOF) as a function of Pd particle size, normalized by the total number of Pd surface atoms (- - -, ☆) and normalized by the total number of Pd surface atoms within incomplete (111) facets (●, ▲). Arrows on the left indicate the TOF of Pd(111) and Pd(110) single crystals under identical reaction conditions.

higher). This corroborates the assumption that the reaction occurred on (111) surface sites and also supports the structure model of a truncated cubo-octahedron with incomplete terraces.

For Pd particles <4 nm, the normalization was not straightforward, because these particles no longer had well-defined (large) (111) terraces. The particles were highly defective, and the exact surface structure was unknown, because STM did not allow a clear characterization of the smallest particles. Nevertheless, normalizing the catalytic activity (molecules converted/s) of Pd particles <4 nm with the number of surface atoms (assuming cubo-octahedra) led to TOF values approaching those of the open Pd(110) single crystal (Fig. 3b). Most likely, although the number of surface sites for diene adsorption was not high, for very small Pd particles, the relative greater abundance of surface defects (low-coordinated sites) may allow for an enhanced hydrogen perforation, giving rise to greater-than-expected activity.

4. Conclusion

UHV-grown Pd–Al_2O_3 model catalysts were used to examine size effects in the selective hydrogenation of 1,3-butadiene at atmospheric pressure at 373 K. Using the common procedure to normalize rates by the total number of Pd surface atoms resulted in a particle size dependence, in agreement with reports for technical catalysts. In contrast, considering Pd atoms within incomplete (111) terraces as active sites (and using their number for rate normalization) led to a particle size-independent reaction rate, at least for Pd particles ⩾4 nm. A realistic structure model was suggested based on STM surface characterization of Pd nanoparticles. Furthermore, the TOF of Pd particles ⩾4 nm was in excellent agreement with the TOF of a Pd(111) single crystal, demonstrating that large, well-faceted Pd particles exhibit the behavior of Pd(111). This had been anticipated for many years and here is proven on a *quantitative* basis. Pd particles <4 nm exhibited rather open surfaces and approached the reactivity of a Pd(110) single crystal. Nevertheless, the se-

lectivity of Pd particles toward butenes was still higher than that of Pd single crystals, with the latter producing a higher amount of *n*-butane. This may be due to a stronger bonding of 1,3-butadiene to Pd nanoparticles. In fact, kinetic measurements on small Pd nanoparticles revealed butadiene-blocking effects on hydrogen adsorption. However, at below some "critical" butadiene coverage, hydrogen was able to (better) perforate the hydrocarbon layer, and the reaction rate increased with time. This "critical" hydrocarbon coverage also was dependent on particle size and most likely reflected a size-dependent binding energy of butadiene.

Acknowledgments

J.S.A. acknowledges support by the Alexander von Humboldt Foundation. The authors thank M. Heemeier and M. Bäumer for STM sample characterization.

References

[1] F.H. Puls, K.D. Ruhnke, US patent 4,260,840 (1981), to Exxon Research & Engineering Co.
[2] H.U. Hammershaimb, J.B. Spinner, US patent 4,774,375 (1988), to UOP Inc.
[3] H. Arnold, F. Döbert, J. Gaube, in: G. Ertl, H. Knözinger, J. Weitkamp (Eds.), Handbook of Heterogeneous Catalysis, Wiley–VCH, Weinheim, 1997, p. 2165.
[4] Á. Molnár, A. Sárkány, M. Varga, J. Mol. Catal. A: Chem. 173 (2001) 185.
[5] T. Ouchaib, J. Massardier, A. Renouprez, J. Catal. 119 (1989) 517.
[6] B.K. Furlong, J.W. Hightower, T.Y.-L. Chan, A. Sarkany, L. Guczi, Appl. Catal. A: Gen. 117 (1994) 41.
[7] J. Massardier, J.C. Bertolini, A. Renouprez, Proceedings of the 9th International Congress on Catalysis, Calgary, 1988, p. 1222.
[8] J. Silvestre-Albero, G. Rupprechter, H.J. Freund, J. Catal. 235 (2005) 52.
[9] H. Conrad, G. Ertl, J. Koch, E.E. Latta, Surf. Sci. 41 (1974) 435.
[10] J.P. Boitiaux, J. Cosyns, S. Vasudevan, Appl. Catal. 6 (1983) 41.
[11] B. Tardy, C. Noupa, C. Leclercq, J.C. Bertolini, A. Hoareau, M. Treilleux, J.P. Faure, G. Nihoul, J. Catal. 129 (1991) 1.
[12] H.-J. Freund, M. Bäumer, H. Kuhlenbeck, Adv. Catal. 45 (2000) 412.
[13] H.J. Freund, M. Bäumer, J. Libuda, T. Risse, G. Rupprechter, S. Shaikhutdinov, J. Catal. 216 (2003) 223.
[14] G. Rupprechter, Annu. Rep. Prog. Chem. C 100 (2004) 237.
[15] J. Silvestre-Albero, G. Rupprechter, H.J. Freund, Chem. Commun. (2006) 80.
[16] M. Morkel, G. Rupprechter, H.-J. Freund, Surf. Sci. Lett. 588 (2005) L209.
[17] A. Doyle, S. Shaikhutdinov, H.-J. Freund, Angew. Chem. Int. Ed. Engl. 44 (2005) 629.
[18] G. Rupprechter, Phys. Chem. Chem. Phys. 3 (2001) 4621.
[19] M. Bäumer, H.-J. Freund, Prog. Surf. Sci. 61 (1999) 127.
[20] M. Kulawik, N. Nilius, H.-P. Rust, H.-J. Freund, Phys. Rev. Lett. 91 (2003) 256101.
[21] K.H. Hansen, T. Worren, S. Stempel, E. Laegsgaard, M. Bäumer, H.-J. Freund, F. Besenbacher, I. Stensgaard, Phys. Rev. Lett. 83 (1999) 4120.
[22] G.C. Bond, G. Webb, P.B. Wells, J.M. Winterbottom, J. Chem. Soc. (1965) 3218.
[23] A.J. Bates, Z.K. Leszczynski, J.J. Phillipson, P.B. Wells, G.R. Wilson, J. Chem. Soc. A: Inorg. Theor. 14 (1970) 2435.
[24] J.C. Bertolini, P. Delichere, B. Khanra, J. Massardier, C. Noupa, B. Tardy, Catal. Lett. 6 (1990) 215.
[25] A. Valcarcel, A. Clotet, J.M. Ricart, F. Delbecq, P. Sautet, Surf. Sci. 549 (2004) 121.
[26] F. Mittendorfer, C. Thomazeau, P. Raybaud, H. Toulhoat, J. Phys. Chem. B 107 (2003) 12287.
[27] P. Sautet, J. Paul, Catal. Lett. 9 (1991) 245.
[28] R. Van Hardeveld, F. Hartog, Surf. Sci. 15 (1969) 189.